SECTION A.I. SITE CHARACTERIZATION
40 CFR 146.82(a)(2), (3), (5), and (6)

MONTEZUMA NORCAL CARBON SEQUESTRATION HUB

Facility Information

Facility name: Montezuma NorCal Carbon Sequestration Hub
IW-A1

Facility contact: Jim Levine, Managing Partner
2000 Powell Street, Suite 920
Emeryville, CA 94608
Phone: (510) 409-1765
Email: jim.levine@upstream.us.com

Well location: Collinsville, Solano County, California
Lat: 38° 5' 7.334" N Long: -121° 51' 30.914" W NAVD 88
Sec 28 T 3 N R 1 E

Table of Contents

List of Tables

List of Figures

A.I.1 REGIONAL GEOLOGY, AND LOCAL STRUCTURAL GEOLOGY [40 CFR 146.82(A)(3)(VI)]

Regional Geology

The proposed injection site is in southwestern Montezuma hills, an area of modestly elevated topography north of the Sacramento River between the reclaimed Delta islands to the east and southeast, and Grizzly Island and Suisun Bay to the west (Figure A.I-1). The Montezuma hills are at the southwestern end of the Sacramento Valley, a subaerial, intermontane basin between the Coast Ranges to the west and Sierra Nevada to the east. The modern Sacramento Valley evolved from an ancestral Mesozoic-Tertiary marine forearc basin that formed above a long-lived, east-dipping subduction zone beneath western California (Ingersoll and Dickinson, 1981). Over the past approximately 28 million years, plate convergence and subduction have been progressively replaced by transcurrent motion and strike-slip faulting in western California, leading to shoaling of the marine basin, uplift of the Coast Ranges to the west, and a transition to continental fluvial deposition in the Sacramento Valley (Graham et al., 1983, and references therein).

FIGURE A.I-1. SURFACE FAULTS IN THE MONTEZUMA HILLS STUDY AREA

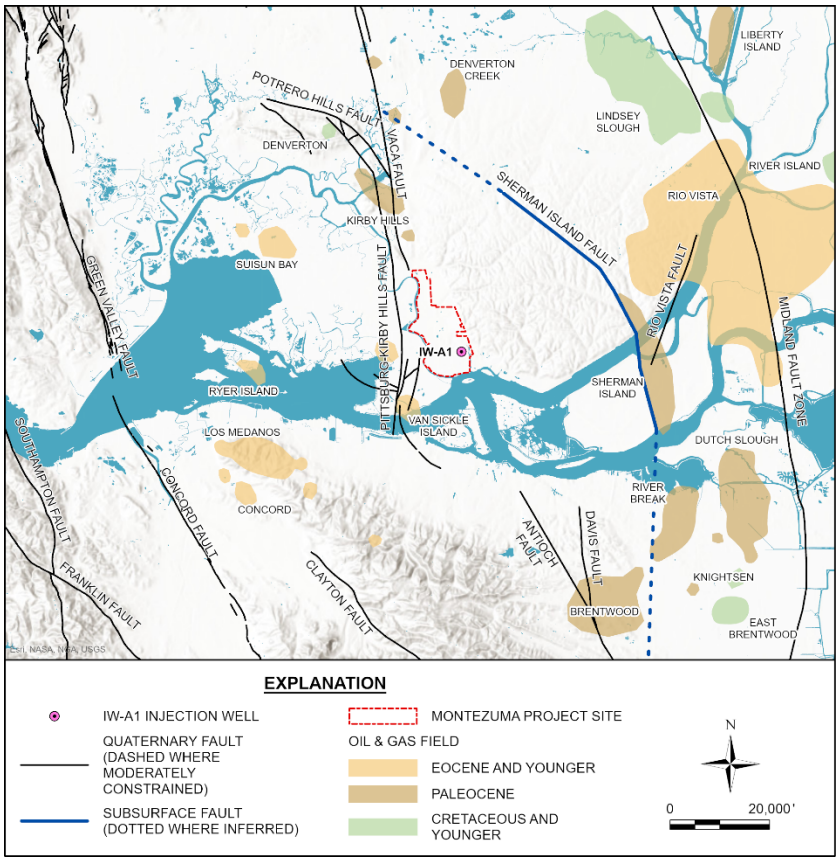

Local Structural Geology

The Montezuma hills approximately coincide with the central part of Rio Vista basin, a north-south-trending extensional sub-basin within the larger forearc basin that formed in early Tertiary time (MacKevett 1992; Krug et al. 1992) (Figure A.I-2). Although the early Tertiary Rio Vista basin is now buried north of the Sacramento River by younger Tertiary and Quaternary terrestrial deposits, an oblique cross-sectional view of the bounding structures and thickened Paleogene marine section in the basin is exposed south of the river in the northeast-dipping backlimb of Mount Diablo anticline. From inspection of this natural, map-scale cross section, the Midland and Kirby Hills fault zones form the eastern and western margins, respectively, of the Rio Vista basin (Figures A.I-1 and A.I-2). Both structures were originally normal faults, and they can be traced in the subsurface of Rio Vista basin southward across the river into the exposed stratigraphic section on the northern flank of Mt. Diablo. The structure correlative to the Kirby Hills fault south of the river is the Kirker fault, which is exposed in the Los Medanos hills between the cities of Pittsburg and Concord. These faults are both active faults and the Kirby Hills fault has evidence of Holocene deformation.

FIGURE A.I-2. EAST-WEST STRATIGRAPHIC CROSS SECTION THROUGH THE MONTEZUMA HILLS. LIGHT YELLOW FORMATIONS ARE RESERVOIR SANDS

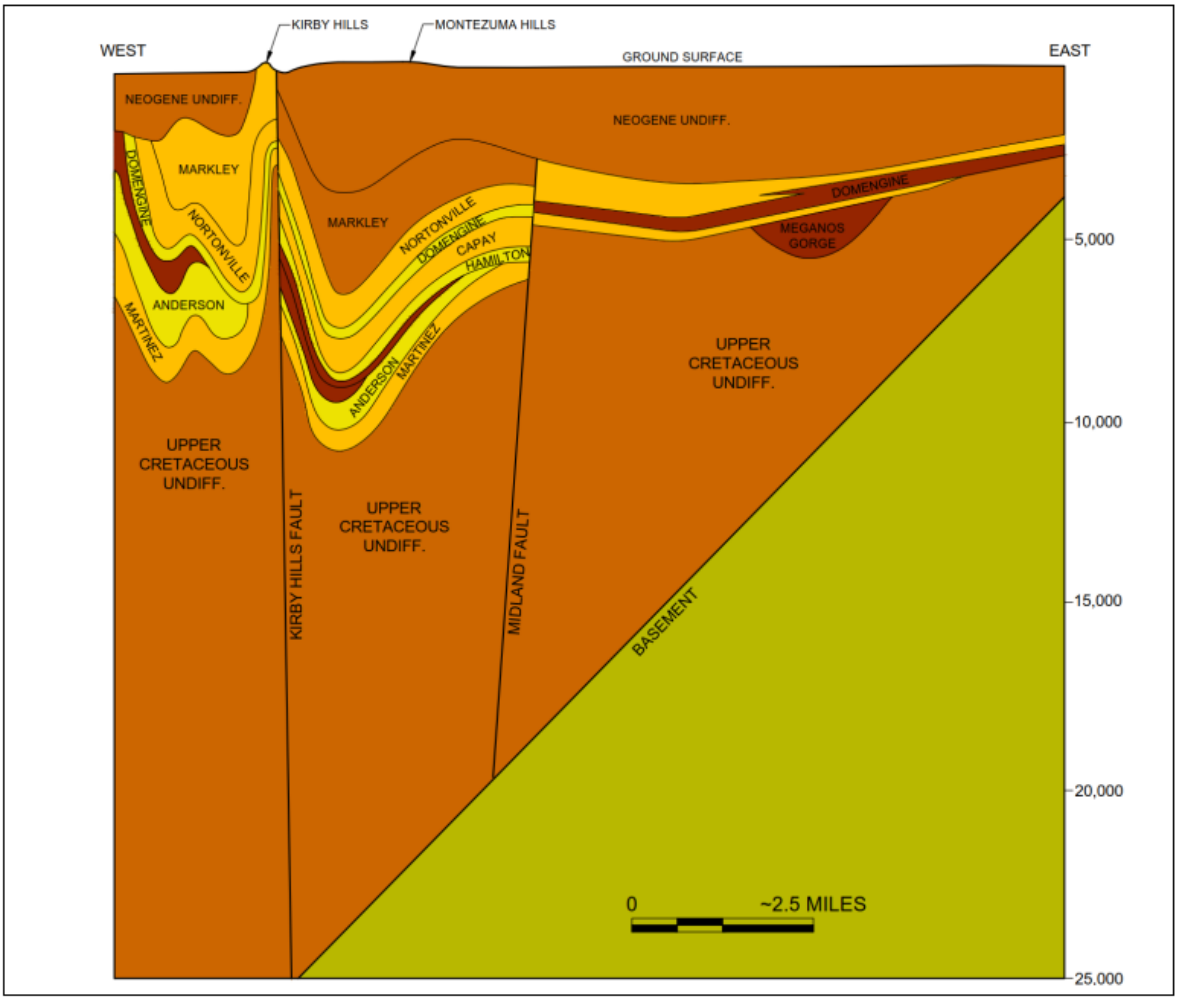

Within the Rio Vista Basin, there is one major fault. The Sherman Island fault is a secondary antithetic normal fault to the Midland fault and terminates westward against the Kirby Hills fault zone (Krug et al., 1992). The Sherman Island fault is mapped west of and subparallel to the Midland fault and interpreted to dip moderately to steeply east (DOGGR, 1982b).

The Paleogene growth section in the Rio Vista basin contains the principal units for injection and confinement. The Anderson sandstone is the planned reservoir for IW-A1, but the Hamilton and Domengine sands are potential future injection intervals as the proposed CO_2 hub expands in size. The confinement zones include the Nortonville Shale (above the Domengine), the Capay Shale (between the Domengine and the Hamilton sandstones), the Meganos/Upper Martinez shale (between the Hamilton and the Anderson sandstones) and the Lower Martinez shale (below the Anderson). A more detailed description of injection intervals and confining zones is provided in subsequent paragraphs within this template for the application.

Paleogene growth strata in the hanging walls of the main and subsidiary normal faults of the Rio Vista basin are exposed on the northern flank of Mt. Diablo (Sullivan et al., 2021a; 2021b), and support interpretation of open-hole logs and other subsurface data from gas exploration in Rio Vista basin (Pasquini and Milligan 1967; DOGGR, 1982; Krug et al. 1992, and references cited therein) for early Tertiary extension and subsidence in the hanging wall of the ancestral western California subduction zone (Unruh 2021).

Active subsidence of the Rio Vista basin ended in Eocene-Oligocene time. Normal displacement on the bounding Kirby Hills and Midland faults dies out upsection in or below the Oligocene Markley Formation (Figure A.I-2). The forearc basin gradually shoaled in middle to late Tertiary time with the transition from convergent motion to transcurrent motion along the western California plate boundary, and marine conditions were replaced by subaerial fluvial environments. The Paleogene marine strata in Rio Vista basin currently are buried by about 1 km of Neogene and Quaternary deposits.

Plio-Pleistocene uplift, tilting and shortening along the eastern margin of the northern Coast Ranges elevated the Montezuma hills above the surrounding estuarine areas of the Sacramento-San Joaquin Delta, and locally folded and faulted the buried strata of the Rio Vista basin. Folding of the Neogene unit (Figure A.I-2) and structure contours on key Paleogene markers in the Rio Vista basin indicate that at the top of the primary injection zone, the Anderson sand, the proposed borehole locations close to the axis of an asymmetric south-southeast-plunging syncline that is subparallel to and about 5-7 km east of the Kirby Hills fault (Figure A.I-3). The syncline axis trends south toward the southern tip of the Montezuma hills. The top of granitic or Franciscan basement is estimated to be greater than 6 km.

As shown in Figure A.I-3, the area bounded by the Sherman Island Fault to the East and North, the Kirby Hills fault zone to the west, and the Antioch fault to the south bound a deep syncline. These faults juxtapose the injection zone sands against shales and are traps for gas fields along the faults. The trapping nature of these large faults indicate that they are no-flow boundaries and represent the boundary of our AoR. Note that parts of the Antioch fault interpretation and the intersection of the Sherman Island fault with the Kirby Hills fault zone have not been imaged and will be updated with a 3D seismic survey prior to drilling the stratigraphic test well.

In the following paragraphs we provide more detail on these gas fields, which provide important geologic control and information about the AoR. We have also included a short description of the Rio Vista field, because it is one of the largest gas fields in the country and provides useful data on the reservoir and confining zones.

Rio Vista: The Rio Vista gas field lies on the Midland fault and is one of the largest gas fields in the country, having produced the equivalent of over 100 MMtonnes of natural gas, primarily from the Hamilton and Domengine sands. The withdrawal of gas has left reservoir pressures near the Midland fault at the Rio Vista field at generally less than 10% of virgin pressures, although unproduced sands are still at virgin pressure indicating no pressure communication across the confining shales. The Midland fault acts as part of the trapping mechanism on the west side of the Rio Vista field from which most of the gas (>3.5 TCF) has been produced. While the drive mechanism on the west side is gas drive, on the east side the mechanism is water drive and no pressure depletion is observed again indicating that the Midland fault is a no flow/pressure boundary.

Kirby Hills: The Kirby gas field is the closest gas field north of the proposed location. The center of this field is roughly 6 miles north of IW-A1, producing natural gas from the Domengine and Anderson zones. These intervals are trapped against the Kirby Hills fault, which juxtaposes Upper Cretaceous shales to the west against the reservoir zones. Kirby Hills is currently being used as a gas storage field. During gas withdrawal, reservoir pressures drop to less than 500 psi and during injection they rise to over 2000 psi. At Kirby Hills, measured permeability in the Anderson (~5500 ft subsea) was between 30 and over 600 mD although we expect compaction effects with depth to reduce the permeability in the Anderson interval to about 20 mD at IW-A1.

Sherman Island: The Sherman Island field was created by an antithetic normal fault to the Midland Fault, down-dropped on the northeast side of the fault. The fault again acts as part of the seal as the Midland Fault does at Rio Vista and at Kirby Hills.

Van Sickle Island: The Van Sickle Island gas field has 20 wells in it, 16 of which are only 1-2 miles west of IW-A1. A typical gas well in this field is between 7,500 ft and 8,000 ft deep and produced gas from the Domengine at that depth. As with the other fields, the Kirby Hills fault possibly splays to form part of the trap.

There are also some key dry holes closer to IW-A1 than these fields that provide important geologic control.

Brazos Oil and Gas "Concord Gun Club": Drilled in 1951 to a depth of 7,003 ft. The well bottomed in the Markley Formation, and thus did not reach any of the zones of interest. However, this well does give data on the shallower zones and the base of the USDW (≥10,000 ppm TDS) which was found to be 1,235 ft.

Hershey Oil "McDougal": Cut the Kirby Hill fault near total depth, ending up in Upper Cretaceous Forbes formation rocks (MacKevett, 1992).

McCulloch Oil "GP 1-7" and "Anderson 5":. These wells lie between IW-A1 and the Sherman Island fault. The Anderson 5 well is important because it drilled over 14,000' and bottomed in the Upper Cretaceous, thus seeing all the potential relevant geologic units of potential interest. The "GP" well went to 11,000 ft and also penetrated all zones of interest.

Further north and within or near the center of the syncline are a group of deep wells. These were drilled at depths of 10,000 ft to over 12,000 ft. Krug, et.al. (1992) show in their paper that these wells were drilled on the western side of the syncline. These wells give good control on the thickness of the Anderson zone across the AoR.

Seismic Data

The geologic suitability of the MC project area was previously evaluated by Shell and LBNL as part of a US DOE-supported pilot CO_2 injection project to handle the CO_2 from Shell's refinery in Martinez (Hymes 2010). The pilot project included drilling and formation property testing followed by injection and monitoring of a small amount of CO_2. Based upon those previous efforts, Shell concluded that the site geology was very attractive, with the ability to safely store large volumes of CO_2. Shell's target injection interval was also the Anderson unit although they noted that the Hamilton and Domengine were also attractive. Members of LBNL staff that contributed to this report have also played a significant role in the Class VI EPA application.

A proposed injection well location was selected roughly 3 miles north of the IW-A1 well based on an old 2-D seismic line (Figure A.I-3). The continuous nature of the unit boundaries can be seen as well as the absence of faulting near IW-A1. Also note the thickening between the Hamilton and Massive horizons.

FIGURE A.I-3. 2-D SEISMIC DATA WITH IW-A1 INJECTION WELL PROJECTED NORTH ALONG STRIKE

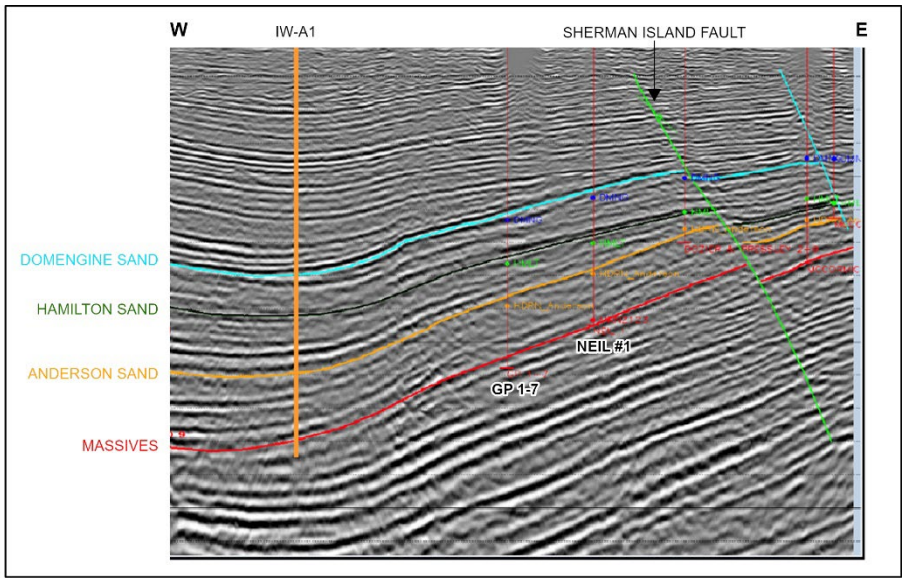

A.I.2 MAPS AND CROSS SECTIONS OF THE AoR [40 CFR 146.82(A)(2), 146.82(A)(3)(I)]

As described above and in Figures A.I-1 through A.I-5, the Area of Review (AoR) is bounded by large faults that are known to be no flow boundaries in gas fields along the faults. Note that there is limited data within parts the AoR, particularly near IW-A1. Once 3D seismic data is available and MW-A1 is evaluated, these maps will be updated. Note that the areal extent of all the formations extend to the boundaries of the AoR. See the Area of Review and Corrective Action Plan for additional maps and cross sections of the AoR.

A.I.3 FAULTS AND FRACTURES [40 CFR 146.82(A)(3)(II)]

A detailed description including maps and cross-sections of the MC site and the associated geologic faults and associated regional structures is provided in the preceding sections of this template document for this application.

A.I.4 INJECTION AND CONFINING ZONE DETAILS [40 CFR 146.82(A)(3)(III)] AND PETROPHYSICAL INFORMATION [40 CFR 146.82(A)(3)(IV)],

Figure A.I-4 shows the predicted formations along with their approximate depths/thicknesses near the IW-A1 location. Figures A.I-5A through A.I-5I provide preliminary contour maps of formation tops that will be updated with 3D seismic data collected for this project. Information about the potential storage reservoirs comes from data sheets for Van Sickle, Kirby Hills, Sherman Island, and Rio Vista gas fields where these formations have produced (State of California, Division of Oil and Gas, Volume 3: Oil and Gas Fields) as well as articles. Information about the confining zones comes from various articles.

FIGURE A.I-4. GENERAL STRATIGRAPHIC COLUMN FOR MC PROJECT AREA

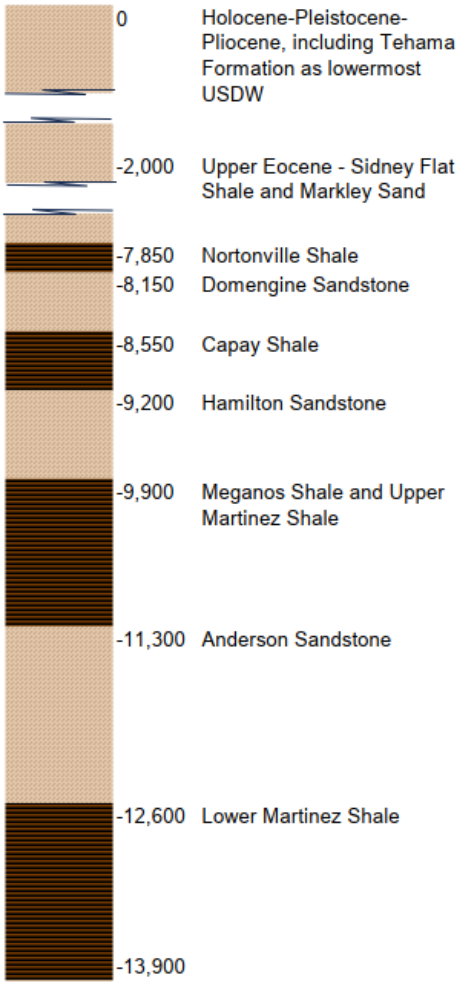

FIGURE A.I-5A. AoR BOUNDARY AND STRUCTURAL CONTOURS – TOP OF NORTONVILLE SHALE

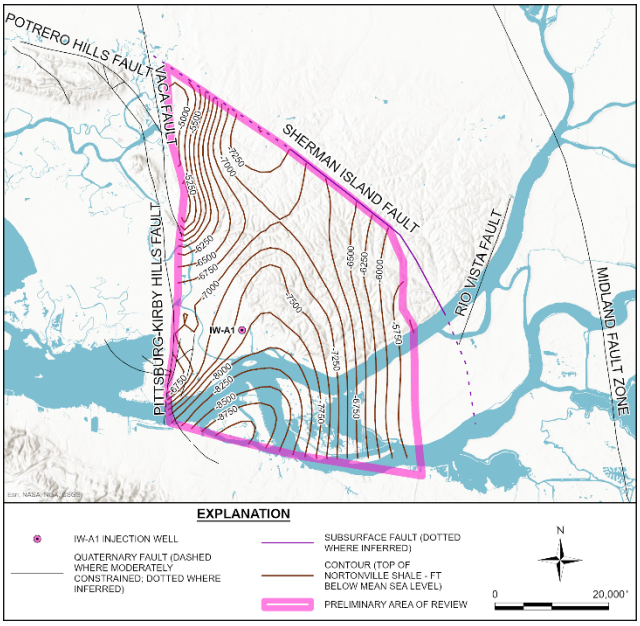

FIGURE A.I-5B. AoR BOUNDARY AND STRUCTURAL CONTOURS – TOP OF DOMENGINE SANDSTONE

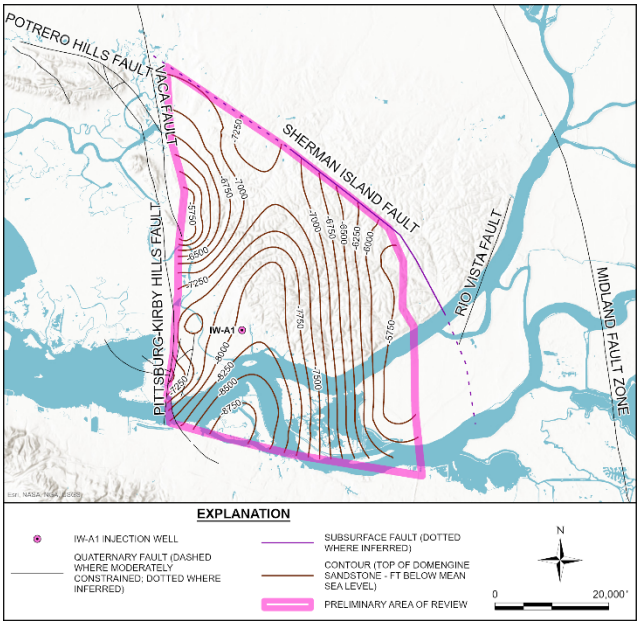

FIGURE A.I-5C. AoR BOUNDARY AND STRUCTURAL CONTOURS – TOP OF CAPAY SHALE

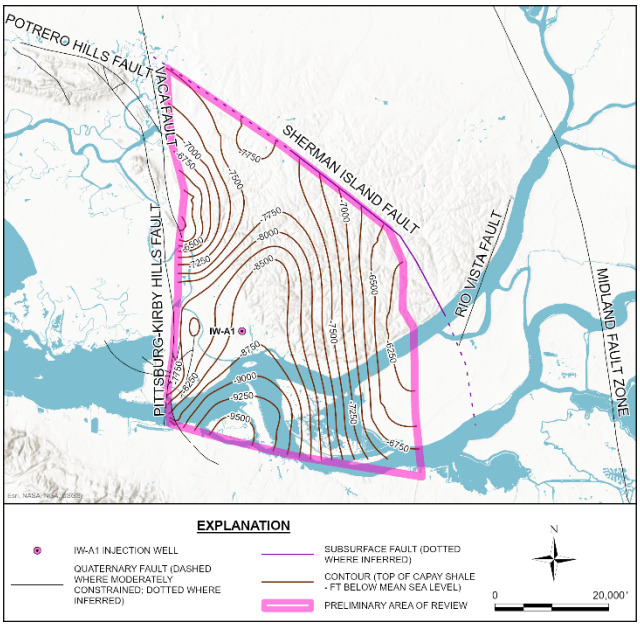

FIGURE A.I-5D. AoR BOUNDARY AND STRUCTURAL CONTOURS – TOP OF HAMILTON SANDSTONE

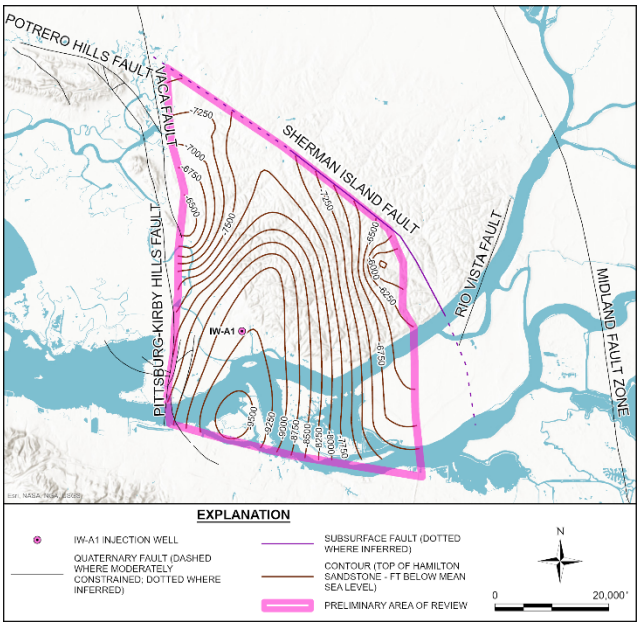

FIGURE A.I-5E. AoR BOUNDARY AND STRUCTURAL CONTOURS – TOP OF MEGANOS SHALE

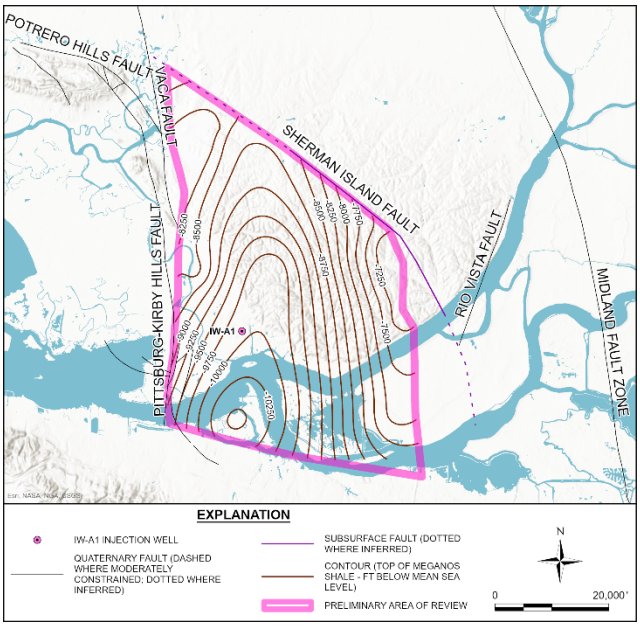

FIGURE A.I-5E. AoR BOUNDARY AND STRUCTURAL CONTOURS – TOP OF UPPER MARTINEZ SHALE

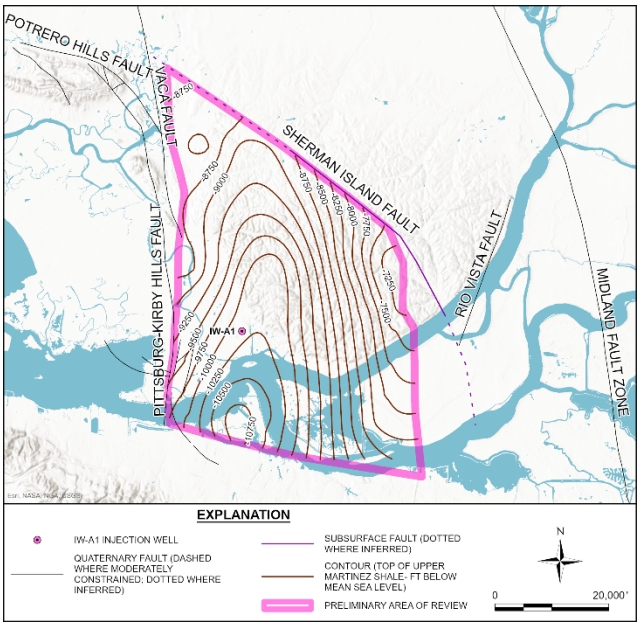

FIGURE A.I-5G. AoR BOUNDARY AND STRUCTURAL CONTOURS – TOP OF ANDERSON SANDSTONE

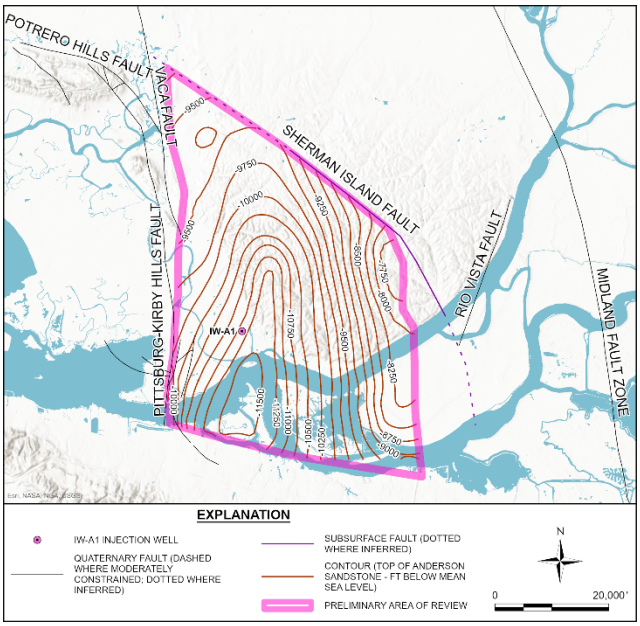

FIGURE A.I-5H. AoR BOUNDARY AND STRUCTURAL CONTOURS – TOP OF LOWER MARTINEZ SHALE

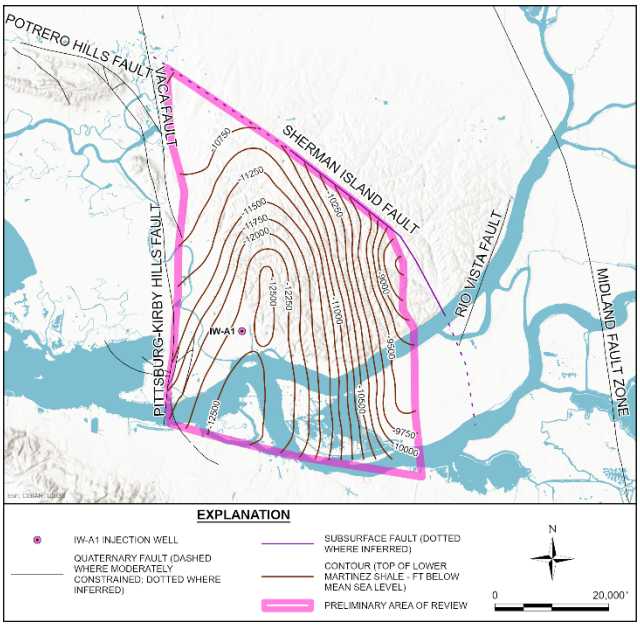

FIGURE A.I-5l. AoR BOUNDARY AND STRUCTURAL CONTOURS – BASE OF LOWER MARTINEZ SHALE

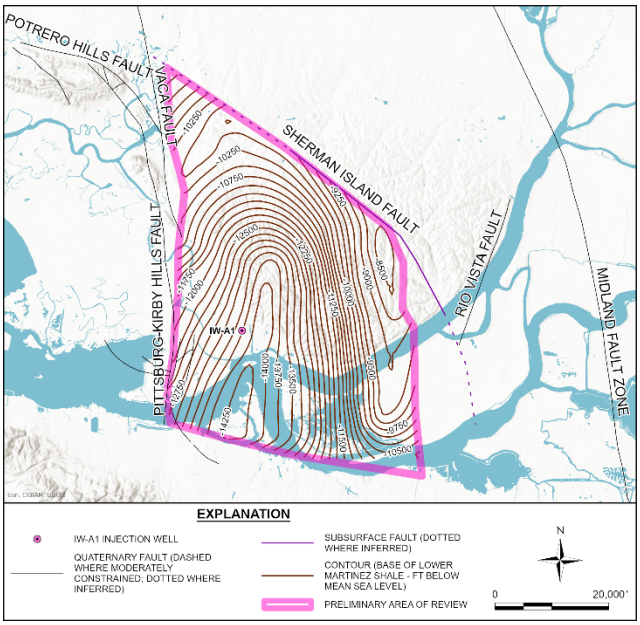

Holocene-Pleistocene-Pliocene [0-2,000 ft]: For the most part, undifferentiated non-marine. Medium to dark gray-green sands, poorly consolidated, volcanic fragments, inclusive of the Tehama Formation. Interbedded soft, silty, massive gray-green and brown clays. Though there is typically a thin zone of very recent materials at and near the surface, a large portion of the lower section from this interval of rock has been named the Tehama Formation. The lowermost USDW zone in the MC project area is considered to occur within this unit at an approximate depth of 2,000 ft subsea (all subsequent depths are registered to sea level and ground level is less than 30 ft above sea level at IW-A1).

Upper Eocene [2000-7850]: Includes the Markley Sand, a fine to medium grained sand of gray-brown color interbedded with carbonaceous brown shales and the Sidney Flat Shale, a massive brown shale. This interval is anticipated to include about 80% shale.

Nortonville Shale [Confining unit] - middle Eocene [7,850-8,150 ft]: Medium to dark gray-brown brittle shale, locally calcareous, with many fossils (forams and diatoms) (Johnson, 1992). This confinement zone is present MacKevett (1992). throughout the study area. This unit is shown as being hundreds of feet thick in all of the gas fields around the area, including Van Sickle and Suisun Bay fields to the west, Sherman Island and Rio Vista to the east, and Kirby Hill to the north.

Domengine Sandstone [Potential future injection zone] - middle Eocene [8,150 -8,550 ft]: This sand unit is one of the most productive zones in the area. An unconformity that eroded the Anderson and Hamilton

sands to the west of the Kirby Hills fault lies at the base of this unit. This formation consists of very fine-medium grained, greenish-gray or white quartz sand, friable, moderately sorted, silty, glauconitic, shell fragments. Fining upwards sequences with two distinct sand units are separated by a more shaley section. Thus, this 400 ft interval is expected to have approximately 270 ft of net permeable zones. Average sand porosity: 20%, range: 16-32%, average sand permeability 40mD, range: 10-100+mD. Thickness of >20 mD sands: 320 +-64 ft. Average total dissolved solids (TDS): 11,000 ppm, range: 10,200-13,000 ppm .

Capay Shale [Confining unit] – lower Eocene [8,550-9,200 ft]: This shale unit is present in most of the project area. However, it is absent in an area along the west side of the Kirby Hill fault zone having been eroded. This unit is composed of light-medium pure gray shale, soft-firm, gummy, moderately cohesive, with very-fine, sub-rounded clear quartz, moderate sorting, with abundant glauconite at the base (Johnson, 1992). As described in the Area of Review and Corrective Action Plan document, computational modeling of future CO_2 plume and pressure evolution during and following injection used literature-based parameters for the Capay shale. The values included 0.01 mD for horizontal permeability, 0.001 mD for vertical permeability, 0.20 for porosity, and a 0.412 for the capillary pressure fitting term λ. The current capillary pressure for supercritical CO_2 versus water is understood to be zero (i.e., negligible separate phase CO_2 within the unit).

Hamilton Sandstone [Potential future injection zone] - lower Eocene [9,200-9,900 ft]: This unit is actually found at the bottom of the Capay Formation, below the Capay Shale. It is described as a light gray, very fine-fine grained, micaceous, carbonaceous sand, friable, clear quartz (Ditzler, 1972). This 700 ft thick interval is estimated to have a net thickness of between 200 to 280 feet at the MC project site. The Hamilton Sand itself has a distinctive shape on the electric logs, with a predominantly shaley and silty sand character near the top gradually becoming more sandy and becoming much more permeable and sandy at the bottom several hundred feet of the zone. Similar to the Capay Shale, this unit is present across most of the project area, however is absent in an area along the west side of the Kirby Hill fault. Average sand porosity: 18%, range: 14-26%, average sand permeability 30mD, range: 10-50md. Thickness of >15 mD sands: 240 +-48 ft. Average total dissolved solids (TDS): 12,000, range: 10,500-13,000 ppm. (State of California, Division of Oil and Gas, Volume 3: Northern California Oil and Gas Fields). As described in the Area of Review and Corrective Action Plan document, computational modeling of future CO_2 plume and pressure evolution during and following injection used literature-based parameters for the Hamilton sandstone. The values included 250 mD for horizontal permeability, 50 mD for vertical permeability, 0.19 for porosity, and a 0.400 for the capillary pressure fitting term λ. The current capillary pressure for supercritical CO_2 versus water is understood to be zero (i.e., negligible separate phase CO_2 within the unit).

Meganos/Upper Martinez Shale [Confining unit] - lower Eocene [9,900-11,300 ft]: Electric logs of the wells closest to the proposed drill site show that there is a thick continuous shale section below the Hamilton

Sand that includes the Meganos Shale and the Upper Martinez Shale. The lower Eocene Meganos shale and the upper Paleocene Upper Martinez shales combine to form a thick confinement zone that is present in the entire project area east of the Kirby Hill fault. The base of the Meganos shale is an erosional unconformity and consists of light-medium, gray to black shale, soft, clayey. The Upper Martinez is a medium-dark brown, firm, hard siltstone, occasionally massive with light-medium gray claystone MacKevett (1992). The total thickness of the Meganos Shale and Upper Martinez Shale formations is expected to be 1,400 ft at the MC project site. As described in the Area of Review and Corrective Action Plan document, computational modeling of future CO_2 plume and pressure evolution during and following injection used literature-based parameters for the Meganos shale. The values included 0.01 mD for horizontal permeability, 0.001 mD for vertical permeability, 0.20 for porosity, and a 0.412 for the capillary pressure fitting term λ. The current capillary pressure for supercritical CO_2 versus water is understood to be zero (i.e., negligible separate phase CO_2 within the unit).

Anderson Sandstone [Targeted injection zone] - middle Paleocene [11,300-12600 ft]: This sandstone unit can be very thick based on well control and seismic data mapped by MacKevett (1992). However, the unit does thin rapidly to the east towards the Rio Vista gas field, where it ends up being missing due to erosion. But, in the heart of the regional syncline, there is a large area in which the sand is at least several hundred feet thick around the outer portion and up to roughly 2,000 feet thick in the center of the regional syncline. In general, the Anderson sandstone is described as a light gray, fine-medium grained, micaceous quartz sand. Logs suggest two main sand packages with a more shaley interval in between. This is the thickest potential injection zone beneath the MC project site, with an expected total thickness of approximately 1,300 ft (MacKevett, 1992) near IW-A1. Average sand porosity: 20%, range: 16-28%, average sand permeability 200mD, range: 20-400mD. Thickness of >50 mD sands: 910 +--182 ft. Average total dissolved solids (TDS): 17,000, range: 13,000-25,000 ppm. (State of California, Division of Oil and Gas, Volume 3: Northern California Oil and Gas Fields). As described in the Area of Review and Corrective Action Plan document, computational modeling of future CO_2 plume and pressure evolution during and following injection used literature-based parameters for the Anderson sandstone. The values included 20 mD and 200 mD for horizontal permeability (two cases modeled), 4 and 40 mD for vertical permeability (two cases modeled), 0.20 for porosity, and a 0.400 for the capillary pressure fitting term λ. The current capillary pressure for supercritical CO_2 versus water is understood to be zero (i.e., negligible separate phase CO_2 within the unit).

Lower Martinez Shale [Confining zone] - lower Paleocene [12,600-13,900 ft]: This shale layer is the lower confinement zone beneath the Anderson sandstone. The description of this unit (Johnson, 1999) is similar to that for the Upper Martinez Shale: medium-dark brown, firm, hard, siltstone, occasionally massive with light-medium gray claystone. There is a base Martinez sand unit named the McCormick sand which is described as a very fine-medium grained, white, quarzitic sand, friable, sorted (Johnson, 1999). However, the thickness of the Lower Martinez Shale should provide suitable confinement for the targeted Anderson injection zone. As

described in the Area of Review and Corrective Action Plan document, computational modeling of future CO_2 plume and pressure evolution during and following injection used literature-based parameters for the Lower Martinez shale. The values included 0.01 mD for horizontal permeability, 0.001 mD for vertical permeability, 0.15 for porosity, and a 0.400 for the capillary pressure fitting term λ. The current capillary pressure for supercritical CO_2 versus water is understood to be zero (i.e., negligible separate phase CO_2 within the unit).

A.I.5 GEOMECHANICAL/Fluid Pressure INFORMATION [40 CFR 146.82(A)(3)(IV)]

Fractures
Based on

1. "Wells within the AoR that intersect the confining and injection zones
2. 2D Seismic data within the AoR
3. Mackevitt (1992)

there are no faults or fractures within the AoR. With future 3D seismic data it may be possible to identify smaller faults and fractures that cannot be identified from existing log and 2D seismic data.

Rock Ductility

The computational modeling described in the Area of Review / Corrective Action Plan portion of this permit application present estimates of geomechanical properties based on literature for the area. The values that characterize rock ductility are repeated here:

TABLE A.I-1. GEOMECHANICAL PROPERTIES (BULK, YOUNG, SHEAR MODULUS)

Unit	Bulk Modulus (GPa)	Young's Modulus (GPa)	Shear Modulus (GPa)
Capay sh	17.5	28.2	11.4
Hamilton ss	19.8	31.2	12.6
Meganos/Upper Martinez sh	21.2	35.6	14.6
Anderson ss	25.2	42.2	17.3
Lower Martinez sh	27.0	47.5	19.7

Rock Strength

The computational modeling described in the Area of Review / Corrective Action Plan portion of this permit application present estimates of geomechanical properties based on literature for the area. The values that characterize rock strength are repeated here:

TABLE A.I-2. GEOMECHANICAL PROPERTIES (ROCK TENSILE STRENGTH)

Unit	Tensile Strength (MPa)
Capay sh	7.3
Hamilton ss	7.5
Meganos/Upper Martinez sh	7.8
Anderson ss	8.1
Lower Martinez sh	8.5

Stress

No stress measurements of the confining or reservoir formation have been performed in the area. An in-situ stress direction of N35E +-12 was obtained from deep earthquake focal mechanisms in the region and borehole breakouts in the Rio Vista field (Unruh, et al, 2019).

Formation Pressure

Estimates of pore pressure and ranges for each of the formations of interest were obtained from mud weights used from Rio Vista to Suisun Bay and are illustrated in Figure A.I-6. The section is normally pressured up until 10,000 ft where pore pressures begin to increase more quickly. Nearby deep wells that penetrate the Anderson UMC "GP" #1-7 and "Anderson" #1-5 both have mud weights below 80 ppm down to 11,000 to 12,000 ft, so we are confident that the Anderson and formations above will be normally pressured. The Anderson injection interval is expected to have a formation pressure ranging from about 6,000 psi at the top to 6,600 psi at the bottom, the upper confining unit is expected to have formation pressures of 5,400 psi at the top and the lower confining unit is expected to have a formation pressure of 7,300 at the bottom. These pressures will be updated after the drilling of MW-A1.

FIGURE A.I-6. PORE PRESSURE ESTIMATES VERSUS DEPTH

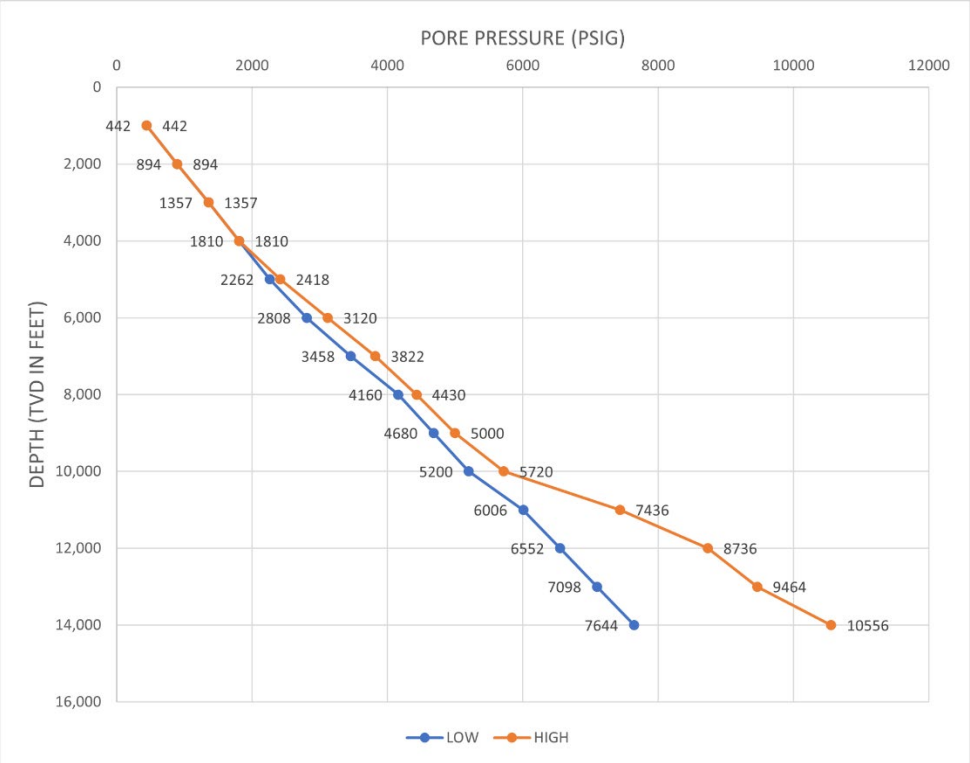

The Area of Review and Corrective Action Plan also presents regional information on the geomechanical and petrophysical properties of the study area. This regional information was used to develop the preliminary modeling and the AoR estimate. The Pre-operational Testing Program describes the plan for obtaining site-specific data on geomechanics and petrophysics of the area. This will include open hole logging as well as soil coring and analysis.

A.I.6 SEISMIC HISTORY [40 CFR 146.82(A)(3)(V)] AND POTENTIAL FOR INDUCED SEISMICITY

A.I.6.1 EARTHQUAKE HISTORY OF MONTEZUMA REGION AND FAULTING

Kirby Hills Fault

The Kirby Hills fault is an active fault that has a history of extremely deep earthquakes in the Montezuma area. Figure A.I-7 is a map showing event locations near the Kirby Hills fault for the period from 1969 and to 2019 (Klotsko, et al, 2023). As shown in the maps, nearly all earthquakes have M<3.0 with hypocenters at depths below 15 km, at least 7 km below the estimated top of basement. The focal mechanisms indicate predominantly right-lateral strike-slip motion. Some, but probably not all the seismicity within the seismic zone are associated with the Kirby Hills fault, although the majority of earthquakes are > 20 km, much deeper than most earthquakes within the San Andreas fault system. This raises the question whether this deep

seismicity is actually related to the shallow Pitttsburg-Kirby fault zone. Other investigators have suggested that the Midland fault, which dips west, may be involved.

FIGURE A.I-7. SEISMICITY HISTORY OF KIRBY HILLS FAULT AREA (1969 - 2014)

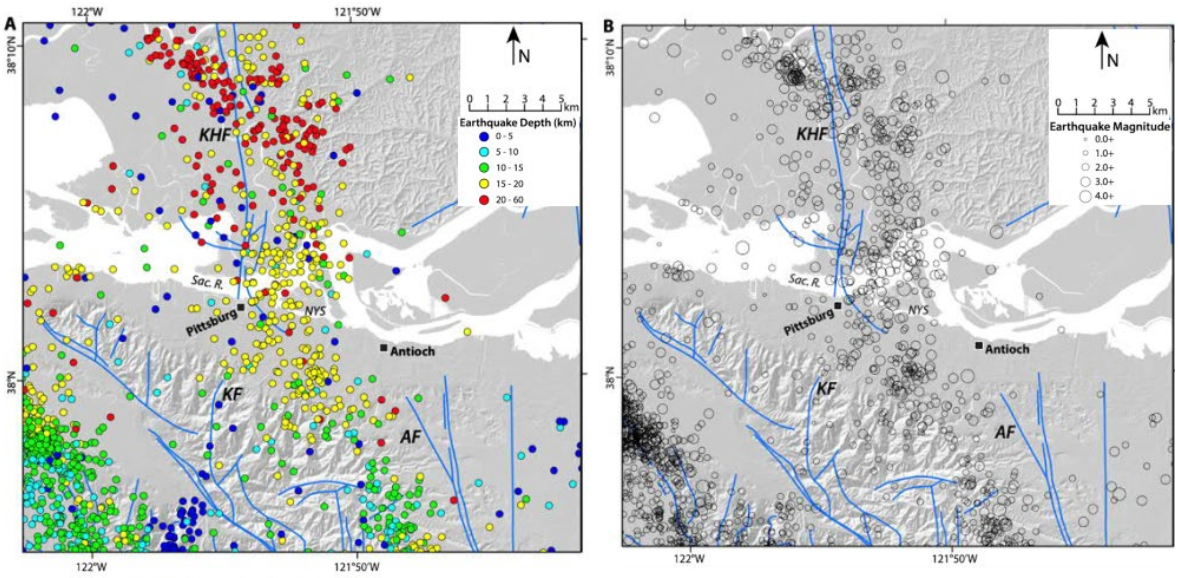

(A) Earthquake depth in kilometers (B) Earthquake magnitude

KHF - Kirby Hills Fault; KF Kirker Fault; AF Antioch Fault; Sac. R. - Sacramento River; NYS New York Slough

USGS and CGS, 2020; Horton et al., 2017

The only large earthquake observed in the area was an (M~6) near Antioch in 1889. It is unknown where the hypocenter was located or even if it was on the Kirby Hills fault.

The Kirby Hills fault strikes roughly N/S and based on the deep hypocenters is assumed to dip about 75 degrees E. In the sedimentary section, the fault zone expands into numerous faults believed to be a flower structure (MacKevett,1992). At the surface the fault zone is about 0.5 km wide and there is evidence of Holocene deformation.

Sherman Island Fault

As shown in Figure A.I-4, the Sherman Island fault is inactive as it terminates near the Neogene boundary.

A.I.6.2 INDUCED SEISMICITY

Induced Earthquakes from Pressure Diffusion

Elevated pore pressures that travel from injection wells to a critically stressed fault via pressure diffusion can initiate slip by reducing the effective pressure, weakening the fault (Walsh and Zoback, 2015). Over the past 15 years in Oklahoma, high volume water disposal wells have induced large (M>5.0) earthquakes in basement

rocks, often miles away from large volume injection wells. Wastewater is injected in the Arbuckle aquifer (which sits on top of basement) resulting in pressure perturbations that diffuse out into the aquifer and then down vertical faults into the basement. Prior to 2009, Oklahoma operators injected water at much lower rates and pressures and there were few induced earthquakes of a detectable magnitude. Beginning around 2009, large scale fracking and horizontal wells generated much larger volumes of wastewater and induced earthquakes increased in frequency. After the Pawnee M=5.8 earthquake the State of Oklahoma directed injection well operators to stop injection if an earthquake of M=4 or greater occurred within 6 miles of an injection well, and to reduce injection volumes if that earthquake occurred between 6 and 10 miles of the injection well. Earthquake magnitudes and frequencies dropped precipitously after the directive began in 2016-2017.

Small Induced earthquakes (M<2, White and Foxall, 2016) related to CO_2 injection have been created by a similar mechanism. The seismic networks monitoring the demonstration CCS project near Decatur, Illinois, recorded about 10,000 events in the magnitude range -2 to 1 from 2011 to 2014 when injection volumes were ~1 MMtonnes/year. Like the Arbuckle injection zone in Oklahoma, the Mt. Simon injection zone in Illinois sits on top of faulted basement and the induced seismicity mechanism is believed to be similar. When the injection zone was moved up away from the basement, induced earthquakes were reduced. A similar pattern of injection zone proximity to basement and frequency of induced earthquakes was observed in Oklahoma.

Induced earthquakes from a Poro-elastic Mechanism

Earthquakes have also been induced from pressure *reduction* due to oil and gas production (Segall, 1989, Sukale 2009). Given that negative fluid pressure changes should *increase* stress and make faults stronger, another mechanism for induced earthquakes called poro-elastic stress transfer was proposed in these papers. In poro-elastic stress transfer, the increased pressure caused by the injection zone radiates a poro-elastic response in the formation in all directions and travels farther and more rapidly than fluid pressure, which stays within the reservoir if there are confining layers above and below. Poro-elastic stress travels with velocities that are a small fraction (<1%) of elastic wave velocities, so the poro-elastic waves reach the hypocenter within minutes to hours depending on the distance between the pressure perturbation and the hypocenter. Unlike pressure diffusion, impermeable layers do not completely impede stress transfer.

An example of what are believed to be poro-elastic stress induced earthquakes due to wastewater injection is shown in Zhai, et al. (2021). The Delaware Basin of West Texas has experienced an increase in earthquake activity that has produced several M>5.0 earthquakes within the last three years. The Delaware Basin has also seen an increase in water disposal volumes in recent years. However, unlike Oklahoma, the injection zone is far above the basement, and there are permeability barriers between the injection zone and the earthquake

hypocenter depths. Consequently, pressure diffusion is unlikely to be the mechanism for inducing deep seismicity here.

Preliminary Assessment of CCS Induced Seismicity Potential at Montenzuma Hills Site

The Montezuma site is quite different from the examples above.

1. The Montezuma injection interval is 2-3 miles above top of crystalline basement, and 8-12 miles above seismicity in the area.
2. The confining units are impermeable thick, continuous shales with an additional 2-3 miles of largely shale confining zones separating the reservoir from the basement.
3. All the major faults in the area (Kirby Hills, Midland, and Sherman Island) are known from gas production adjacent to the fault to be impermeable.
4. None of the huge volumes of gas withdrawn in the area (over 4 TCF) has affected pressures away from the fields nor was any induced seismicity or change in active seismicity due to gas production been observed indicating that poroelastic effects are insufficient for creating seismicity either in the reservoir or the basement.

Consequently, the risk of CO_2 injection causing large (M>4.5) events is negligible and if any seismicity is detected it is most likely to be unfelt small events near the reservoir interval and the injection well.

Small faults and fractures below the resolving power of 3D seismic data (25-50 ft of throw) cannot be ruled out in the AoR and could slip due to pressure changes in the reservoir, or changes in rock properties due to the plume. However, these earthquakes are highly unlikely to cause any damage.

Potential for Damage to Injection Wells or Compromise of Seals from Natural or Induced Seismicity

The report of Pratt, et al. (1978), concludes that there are virtually no examples of underground damage from the vibrations produced by earthquakes of any magnitude. Even the 1964 Alaska quake had no damage to underground structures including oil and gas wells in Cook Inlet. The report also states that underground examples of well damage are invariably correlated with fault displacement. In the Montezuma AoR, any fault slip in the plume region (if there are any faults at all), will be far less than the thicknesses of the bounding shales and the seals will not be compromised. Even a small fault intersecting the well is highly unlikely, particularly because the well will be sited using 3D seismic data. Should one be encountered during drilling, the well will be sidetracked to avoid the fault.

A.I.7 HYDROLOGIC AND HYDROGEOLOGIC INFORMATION [40 CFR 146.82(A)(3)(VI), 146.82(A)(5)]

The Montezuma Hills are low-lying, reaching a maximum elevation of less than 90 meters (300 feet) above sea level. The hills drain predominantly to the Sacramento River to the southeast. The only perennial streams in the hills occupy some of these drainages. Minor seasonal streams drain the margins of the hills to the north and west. The water table depth in the Montezuma Hills may increase to as much as 30 m (100 ft) beneath the highest ridges (elevation 90 m) in the central portion of the hills, however, there are perennially wet drainages in this central area at an elevation of approximately 60 m (200 ft).

The maximum horizontal gradient occurs from the center to the edge of the Montezuma Hills, a minimum distance of 6.5 km (4 mi). Assuming the water table elevation to be 60 m (200 ft) at the center and sea level at the edge, this yields a gradient of about 0.01. Gradients outside this area can be expected to be much less due to the flat topography and pervasiveness of perennial water channels.

The average hydraulic conductivity in the Sacramento Valley aquifer is 0.9 m d^{-1} (3 ft d^{-1}) (Williamson et al., 1989). Combining this with the maximum gradient of 0.01 and an estimated effective porosity of 25% yields an estimated maximum linear groundwater velocity of 15 m yr^{-1} (50 ft yr^{-1}). While the hydraulic conductivities may be higher or lower, they are probably similar to the Sacramento Valley average. Water pressures are hydrostatic from the water table down to the Cretaceous Delta Shale.

The main USDW in the area is the thick gravel-rich Tehama Formation, which is an approximately 610 m (2000 ft) thick aquifer that extends to about 915 m (3000 ft) below the surface. The Tehama Formation is a sedimentary rock unit that is primarily composed of sandstone, siltstone, shale, and conglomerate. It is part of the larger Cenozoic sedimentary sequence within the Sacramento Basin. The deposition of the Tehama Formation began during the late Cretaceous period, approximately 80 to 70 million years ago, and continued into the early Tertiary period. It represents a time when the Sacramento Basin was submerged beneath a shallow marine environment.

The Tehama Formation consists of layers of marine and non-marine sediments that were deposited in various environments, including coastal plains, estuaries, and shallow marine environments. The deposition of sediments was influenced by factors such as sea-level changes, tectonic activity, and sediment supply from nearby mountain ranges. The sandstone and conglomerate layers within the Tehama Formation indicate the presence of ancient river systems that transported and deposited coarse sediments. These sediments likely originated from the uplifted Sierra Nevada Mountains and other nearby sources. The siltstone and shale layers, on the other hand, represent finer-grained deposits that settled in calm marine or estuarine environments.

This shallow freshwater aquifer is separated from the underlying Tertiary and Upper Cretaceous deep saline formations by a thick, low permeability aquitard of clay-rich volcanoclastic sandstones. All CO_2 injection targets lie well below this aquitard and therefore there is good low permeable separation between the USDWs and the deep saline formations in the area.

A.I.8 GEOCHEMISTRY [40 CFR 146.82(A)(6)]

The amount of geochemical data available at present on the Montezuma Carbon Project is limited. Much of the lack of data is due to the rules of the State of California and how much of the data gained during the well drilling into the deep formations can be kept confidential and not released to the public. However, the testing & and monitoring efforts to be undertaken for this project will work to fill those data limitation, and much more will be known.

The Domengine zone is the only interval that has a geochemistry paper written about it. That paper is by Todd and Moore (1968), and it is entitled "Petrology of Domengine Formation (Eocene) at Potrero Hills and Rio Vista, California" and was published in the Journal of Sedimentary Petrology. They describe the formation as a feldspathic subgraywacke unit that includes clayey sandstone, sandy siltstone, and silty shale. It accumulated under primarily transgressive marine conditions. This study was done from both outcrop samples in the Potrero Hills and from core samples in the Rio Vista gas field, located some 15 miles apart. Both of these areas are either in or near the MC project AoR. It was found that most of the Domengine is comprised of quartz, with 60%-70% being common quartz. The most common clay mineral was kaolinite. The most common rock fragments were metamorphics, which included quartz-muscovite schist, argillite, and aphanitic and plagioclase lath-bearing varieties. The average grain had subangular roundness and was between 0.09 and 0.19 mm in size.

A.I.9 SITE SUITABILITY [40 CFR 146.83]

The proposed injection site was previously studied for geologic suitability by Shell and LBNL as part of a DOE-supported pilot CO_2 injection project to handle the CO_2 from Shell's refinery in Martinez (Hymes, 2010). The pilot project proposed with drilling and formation property testing followed by injection and monitoring of a small amount of CO_2 into the Anderson sand. Based upon those previous efforts, Shell concluded that the site geology was very attractive, with the ability to safely store large volumes of CO_2. The reservoir zones were thick, porous, continuous sands and the relevant confining units are thick, laterally continuous shale units known to be flow and pressure barriers in nearby gas fields. However, at that time the economics for a carbon capture project of this potential scale were not justified. Those economics and governmental support have changed in recent years.

In the development of this proposal, we have built off the previous Shell/LBNL study, focusing it on our specific acreage in the Montezuma hills. We have performed additional studies of reservoir properties, incorporating not only well logs and seismic, but drilling and production data from nearby wells and gas fields and newer geologic studies of the area.

Using the geological, production, and geophysical information, we created a geologic and physical property model for plume and pressure front simulations which showed:

1. A single vertical well could inject one MMtonnes/year for over 40 years into the 1,300 ft thick Anderson sand reservoir located at 11,300 ft.
2. The plume extent is approximately 1.3 km in radius after 100 years and pressure increases of less than 1.7 MPa are created on the sealing faults to the east and west of the injection well.
3. There is enough acreage at the site to put in at least three Anderson vertical injection wells on the current acreage.
4. Other sand units (Domengine, Hamilton and potentially others), could potentially store comparable amounts of CO_2, and we believe that overall the site has a most likely storage estimate of over 250 MMtonnes of CO_2 at injectivity rates of over 5 MMtonnes per year.
5. Even if pessimistic forecasts of reservoir parameters are used, the site has storage potential of over 80 MMtones at rates of over 2 MMtonnes per year.

Risks of Leaks

There is a negligible risk of leakage into shallow units due to injection. First, the confining units are thick, continuous, clay-rich shales that extend in intervals for thousands of feet above the injection interval. Second, production data from nearby gas fields has demonstrated that the reservoirs are not in communication. Third, the major faults in the area (Kirby Hills, Midland, and Sherman Island) are known from gas production to be traps. Fourth, the plume only extends 1.3 km away from IW-A1 and there is no evidence of faulting near the injection well, and the shales above and below the reservoir are continuous far past the modeled plume extent.

A.I.10 REFERENCES

Burroughs, E., 1967, Rio Vista gas field: California Division of Oil and Gas, Summary of Operations: California Oil Fields, vol. 53, No. 2 – Part 2, p. 25-33.

California Division of Oil and Gas, 1982, California oil and gas fields, Northern California: Publication TR10, vol. 3. data sheets, pages of fields as follows: Denverton Creek, p. 74-75; Kirby Hill, p. 128-129;

Kirby Hill North, p. 130-131; Potrero Hills, p. 220-221; Rio Vista, p. 236-239; Ryer Island, p. 249-250; Sherman Island, p. 261-262; Van Sickle Island, p. 303-304.

Cherven, V.B., 1983, Mesozoic through Paleogene evolution of the Sacramento basin, California, in Cherven, V.B. and Graham, S.A., eds., Geology and Sedimentology of the Southwestern Sacramento Basin and East Bay Hills: Field Trip Guidebook, Pacific Section, Society of Economic Paleontologists and Mineralogists, Los Angles, p. 21-31.

Crane, R.C., 1995, Geology of the Mt. Diablo region and East Bay hills, in Sangines, E.M., Andersen, D.E., and Buising, A.V., eds., Recent Geologic Studies in the San Francisco Bay Area: Pacific Section SEPM (Society for Sedimentary Geology), Volume 76, p. 87-114.

Ditzler, Clark C., 1972, Sherman Island Gas Field, in Selected Papers present to San Joaquin Geological Society, Volume 4, p. 21-25.

Division of Oil, Gas and Geothermal Resources (DOGGR), 1982a, California Oil and Gas Fields, Volume III – Northern California; Contour maps, cross sections and data sheets: California Department of Conservation, 330 p. (available from *http://repository.usgin.org/category/place-keywords/california*; last accessed 4/8/22)

Division of Oil, Gas, and Geothermal Resources (DOGGR) 1982b, Sherman Island gas field, in California Oil and Gas Fields, vol. III, Northern California: California Department of Conservation, Division of Oil and Gas, publication TR10.

Graham, S.A., Gavigan, C., McCloy, C., Hitzman, M., Ward, R., and Turner, R., 1983, Basin evolution during the change from convergent to transform continental margin: an example from the Neogene of California, in Cherven, V.B., and Graham, S.A., eds., Geology and Sedimentology of the Southwestern Sacramento Basin and East Bay Hills: Field Trip Guidebook, Pacific Section, Society of Economic Paleontologists and Mineralogists, Los Angles, p. 101-118.

Hector, Scott, 2000, Stratigraphic Variations in the Paleocene and Upper Cretaceous Sands and their effect on gas entrapment, Denverton Creek gas field, Sacramento Valley, (abstract), AAPG Search and Discovery Article #90911, Pacific Section and Western Region, Society of Petroleum Engineers, Long Beach, CA.

Hector, Scott, 2014, Lindsey Slough Gas Field: History of Development, (abstract), Pacific Section AAPG, SPE, and SEPM Technical Conference, Bakersfield, CA.

Hector, Scott, 2014, Rio Vista Gas Field: History of Development, (abstract), Pacific Section AAPG, SPE and SEPM Technical Conference, Bakersfield, CA.

Hymes, E., 2010, Northern California CO2 Reduction Project Final Scientific/Technical Report

Ingersoll, R. V., and Dickinson, W. R., 1981, Great Valley Group (sequence), Sacramento Valley, California, in Frizzell, V., ed., Upper Mesozoic Franciscan rocks and Great Valley sequence, central Coast ranges, California (Annual Meeting, Pacific Section SEPM field trips 1 and 4): Pacific Section, Society of Economic Paleontologists and Mineralogists, p. 1–33.

Johnson, D. S., 1992, Rio Vista Field, in Beaumont, Edward A. and Foster, Norman , compilers, Structural Traps III Tectonic Fold and Fault Traps: Treatise of Petroleum Geology: Atlas of Oil and Gas Fields, American Association of Petroleum Geologists, p. 243-264.

Johnson, D. S., 1990, Rio Vista gas field – USA, Sacramento Basin, Calif. in Foster, N. H., and Beaumont, E.A., eds., Atlas of oil and gas fields, Structural Traps III, AAPG. Treatise of Petroleum Geology, Atlas of Oil and Gas Fields, Tulsa, Oklahoma, U.S.A.

Klotsko, Shannon, Jillian Maloney, and Janet Watt. 2023, Shallow deformation on the Kirby Hills fault, Sacramento–San Joaquin Delta, California (USA), revealed from high-resolution seismic reflection data and coring in a fluvial system. *Geosphere*.

Krug, E.H., Cherven, V.B., Hatten, C.W., Roth, J.C., 1992, Subsurface structure in the Montezuma Hills, southwestern Sacramento basin, in Cherven, V.B., and Edmondson, W.F., eds., Structural Geology of the Sacramento Basin: Volume MP-41, Annual Meeting, Pacific Section, Society of Economic Paleontologists and Mineralogists, p. 41-60.

Lodi Gas Storage, LLC, 2007, Kirby Hill Phase II Natural Gas Storage Facility – Initial Study and Subsequent Mitigated Negative Declaration.

MacKevett, N.H., 1992, The Kirby Hills fault zone, in Cherven, V.B., and Edmondson, W.F., eds., Structural Geology of the Sacramento Basin: Volume MP-41, Annual Meeting, Pacific Section, Society of Economic Paleontologists and Mineralogists, p. 61-78.

Myer, L., L. Chiaramonte, T. M. Daley, D. Wilson, W. Foxall, J. H. Beyer, 2010, Potential for Induced Seismicity Related To The Northern California CO2 Reduction Project Pilot Test, Solano County, California , LLNL-TR-435831 June 15.

Oldenburg, Curtis M. and Preston D. Jordan, 2017, Long-Term Viability of Underground Natural Gas Storage in California An Independent Review of Scientific and Technical Information, California Council on Science and Technology December.

Pacific Section American Association of Petroleum Geologist, Geology of the Sacramento Basin, Publication No. MP-41, p. 41-60 and p. 61-78.

Pasquini, D.E., and Milligan, H.L., 1967, Correlation Section 15, Sacramento Valley, Suisun Bay to Lodi: Pacific Section, American Association of Petroleum Geologists.

Pepper, Miles W. and Johnson, Dane, 1992, The Midland Fault System, Southern Sacramento Basin, California, in Cherven, V.C., and Edmondson, W.F., eds., Structural Geology of the Sacramento Basin, Pacific Section, American Association of Petroleum Geologists, Publication No. MP-41, p. 27-40.

Pratt, H. R., W. A. Hustrulid, D. E. Stephenson, 1978, Earthquake Damage to Underground Facilities, Environmental Transport Division.

Segall, P., 1989, Earthquakes triggered by fluid extraction, Geology, 17, 942–946.Suckale, J. (2009), Induced seismicity in hydrocarbon fields, Adv. Geophys., 51, 55–106.

Suckale, J. (2009), Induced seismicity in hydrocarbon fields, Adv. Geophys., 51, 55–106.

Sullivan, R., Sullivan, M.D., Dedmon, P., and Edwards, S.W., 2021a, The occurrence and mining of coal and sand deposits in the Middle Eocene Domengine Formation of the Mount Diablo Coalfield, California, in Sullivan, R., Sloan, D., Schwartz, D., and Unruh, J., Regional Geology of Mount Diablo, California: Its Tectonic Evolution on the North American Plate Boundary: Geological Society of America Memoir 217, p. 65-95.

Sullivan, R., Sullivan, M.D., Edwards, S.W., Sarna-Wojicicki, A., Hackworth, R.A., Deino, A.L., 2021b, The mid-Cenozoic succession on the northeast limb of Mount Diablo anticline, California-a stratigraphic record of tectonic events in the forearc basin, in Sullivan, R., Sloan, D., Schwartz, D., and Unruh, J.,

Regional Geology of Mount Diablo, California: Its Tectonic Evolution on the North American Plate Boundary: Geological Society of America Memoir 217, p. 269-303.

Todd, Thomas W. and William A. Monroe**,** 1968, Petrology of Domengine Formation (Eocene), at Potrero Hills and Rio Vista, California: Journal of Sedimentary Research, vol. 38, no. 4, p. 1024-1039.

Unruh, J., 2021, Upper plate deformation during blueschist exhumation, ancestral western California forearc basin, from stratigraphic and structural relationships at Mount Diablo and in the Rio Vista Basin, in Sullivan, R., Sloan, D., Schwartz, D., and Unruh, J., Regional Geology of Mount Diablo, California: Its Tectonic Evolution on the North American Plate Boundary: Geological Society of America Memoir 217, p. 179-200.

Unruh, J., Hitchcock, C., Blake, K., and Hector, S., 2016, Characterization of the Southern Midland Fault in the Sacramento-San Joaquin Delta, in Ferriz, H. and Anderson, R., eds., Applied Geology in California: Association of Engineering Geologists, Special Publication 26, p. 757-776.

Unruh, J.R., and Hector, S.T., 1999, Subsurface Characterization of the Potrero-Ryer Island Thrust System, Western Sacramento-San Joaquin Delta, Northern California: Final Technical Report submitted to the U.S. Geological Survey, National Earthquake Hazards Reduction Program award number 1434-HQ-96-GR-02724, 32 p.

Unruh, J, Wong, I, and Smith, S. (2015), Seismotectonic Characterization of the Coast Ranges-Sierran Block Boundary Zone, California FINAL TECHNICAL REPORT U. S. Geological Survey National Earthquake Hazards Reduction Program.

Walsh, F.R., and Zoback, M.D., 2015, Oklahoma's recent earthquakes and saltwater disposal: Science Advances, v. 1, e1500195, doi:10.1126 /sciadv.1500195.

White, J. A, and Foxall, W., 2016, Assessing induced seismicity risk at CO_2 storage projects: recent progress and remaining challenges. International Journal of Greenhouse Gas Control, vol. 49, p. 413-424. https://doi.org/10.1016/j.ijggc.2016.03.021

Williamson, A.K., Prudic, D. E., and Swain, L. A., 1989, Ground-water Flow in the Central Valley, California. U. S. Geological Survey Professional Paper 1401 -D.

Zhai, G., M. Shirzaei, and M. Manga (2021) Widespread deep seismicity in the Delaware Basin, Texas, is mainly driven by shallow wastewater injection, PNAS, vol. 118, e2102338118.

Zieglar, D. L., and J. H. Spotts, 1978, Reservoir and source-bed history of the Great Valley, California: American Association of Petroleum Geologists Bulletin, vo. 62, p. 813-826.